

## Ionization cross sections for 10–300-keV/u and electron-capture cross sections for 5–150-keV/u ${}^3\text{He}^{2+}$ ions in gases

M. E. Rudd, T. V. Goffe,\* and A. Itoh

*University of Nebraska-Lincoln, Lincoln, Nebraska 68588-0111*

(Received 6 May 1985)

Cross sections for production of positive and negative charge for 10–300-keV/u  $\text{He}^{2+}$  ions on He, Ne, Ar, Kr,  $\text{H}_2$ ,  $\text{N}_2$ , CO,  $\text{O}_2$ ,  $\text{CH}_4$ ,  $\text{N}_2\text{O}$ , and  $\text{CO}_2$  were measured by the transverse-field method. Single- and double-electron-capture cross sections at 5–150 keV/u for the same targets were measured by the method of deflection of different charge-state components of the beam after passing through a known length of target gas. A secondary-emission detector was used to detect the neutral component of the beam. A small least-squares adjustment of the cross sections was made to satisfy the equation  $\sigma_+ = \sigma_- + \sigma_{21} + 2\sigma_{20}$  which follows from conservation of charge.

### INTRODUCTION

The basic processes of electron ejection and charge transfer in atomic collisions are important in a number of areas of research such as plasma and fusion studies, upper-atmospheric work, and radiation detection. Yet, no theoretical or even empirical methods have been devised to calculate cross sections for these processes except for collision velocities that are large compared to the orbital velocities of the target. Even in this case, calculations are not available for heavy atoms or for molecules. Therefore, experimental measurements remain the only way to determine these cross sections in most cases. Such measurements are also needed as a basis for developing new theoretical methods.

To provide a basis for testing theoretical models of electron ejection and charge transfer, it is desirable to have measurements over a wide energy range for a variety of projectiles and targets. Since protons and helium ions are the simplest projectiles, they are of especial interest in this regard. The Born approximation predicts a  $Z_p^2$  dependence of the cross sections on projectile charge for bare nuclei. A comparison of data using  $\text{He}^{2+}$  and proton beams can be used to check this dependence. Tests of this dependence have generally been confined to the higher energies.

While data on electron capture in  $\text{He}^{2+}$  impacts are available for a number of the simpler atomic and molecular targets,<sup>1–11</sup> there are several common gases for which no measurements have been made. Relatively few studies of ionization have been made.<sup>12–15</sup>

In this experiment we have measured  $\sigma_+$  and  $\sigma_-$ , the cross sections for production of positive and negative charge, and  $\sigma_{21}$  and  $\sigma_{20}$ , the cross sections for capture of one and two electrons. These measurements, made for 11 target gases, cover an energy range which spans the maximum in the cross-section curves and extends up to the energy where the Born approximation begins to be accurate.

### EXPERIMENTAL PROCEDURE

The cross sections  $\sigma_+$  and  $\sigma_-$  were measured by the transverse-field method described previously for proton<sup>16</sup>

and singly charged helium-ion<sup>17</sup> measurements. The capture cross sections were measured by electrostatic separation of the various charge components of the beam after it was allowed to pass through a known length of target gas at a measured pressure. The apparatus used in these measurements was previously used to make similar charge-transfer measurements with  $\text{He}^+$  projectiles and is described elsewhere.<sup>17</sup> Typical target-gas pressures used in the present work were  $10^{-4}$  Torr for the capture measurements and  $(1-5) \times 10^{-4}$  Torr for the ionization measurements. Background pressures were about  $2 \times 10^{-7}$  Torr when no target gas was admitted. The pressure used in the ionization measurements was low enough that no correction was made for neutralization of the beam. The resulting error was only about 5% in the worst case and generally much smaller.

Because  ${}^4\text{He}^{2+}$  has the same charge-to-mass ratio as  $\text{H}_2^+$  and since hydrogen is very difficult to eliminate from an ion source, the isotope  ${}^3\text{He}$  was used as the gas from which the projectile ions were made. These ions have a unique charge-to-mass ratio yielding an unambiguously defined beam. We have found by magnetic analysis of the beam that even using an ion-source tube which had never been used with hydrogen, a proton beam was present which constituted about  $\frac{1}{5}$  of the total beam. This indicates that  $\text{He}^{2+}$  data taken using ordinary helium may have a sizable error due to the presence of  $\text{H}_2^+$  in the beam.

Measurements were made using two accelerators over the voltage range of 8.5 to 350 kV which yielded values of energy per unit mass from 5.67 to 233 keV/u. By making a small extrapolation, results are presented for ionization from 10–300 keV/u and for capture from 5–150 keV/u.

### EXPERIMENTAL UNCERTAINTIES

For all measurements the uncertainty in the measurement of the target-gas density was 4%. For the measurement of  $\sigma_+$  and  $\sigma_-$  the beam-current collection and the background correction had uncertainties which varied somewhat with energy but averaged 6% and 3%, respectively. The effective length was known to be better than 1%. These combined to give an 8% uncertainty. For  $\sigma_{21}$

TABLE I. Values of  $\sigma_+$  for  ${}^3\text{He}^{2+}$  collisions. Units are  $10^{-20} \text{ m}^2$ .

Energy (keV/u)	He	Ne	Ar	Kr	H <sub>2</sub>	N <sub>2</sub>	CO	O <sub>2</sub>	CH <sub>4</sub>	CO <sub>2</sub>	H <sub>2</sub> O
10	3.8	9.6	24	39	11	25	28	23	26	33	24
15	4.7	10	27	40	14	28	30	25	30	36	25
20	5.4	10	27	39	15	29	30	26	32	38	25
30	6.0	9.8	26	37	14	28	29	26	32	37	24
40	5.9	9.4	25	36	13	26	27	25	32	36	23
50	5.6	9.0	24	33	12	25	26	24	31	35	23
75	4.9	8.2	21	29	9.8	21	22	21	27	32	20
100	4.3	7.4	19	26	8.4	19	20	19	24	29	18
150	3.4	6.5	16	23	6.7	16	17	16	20	25	16
200	2.8	5.9	14	20	5.4	14	14	15	17	23	14
300	2.1	5.0	12	16	4.1	12	12	12	14	19	12
Unc.	9%	8%	8%	9%	9%	9%	9%	9%	9%	8%	11%

TABLE II. Values of  $\sigma_-$  for  ${}^3\text{He}^{2+}$  collisions. Units are  $10^{-20} \text{ m}^2$ .

Energy (keV/u)	He	Ne	Ar	Kr	H <sub>2</sub>	N <sub>2</sub>	CO	O <sub>2</sub>	CH <sub>4</sub>	CO <sub>2</sub>	H <sub>2</sub> O
10	0.14	1.3	6.2	10	1.1	7.5	7.4	7.9	8.0	13	5.5
15	0.37	1.8	8.8	13	2.0	9.2	9.7	9.7	11	16	7.3
20	0.61	2.3	10	15	3.1	11	12	11	14	18	8.8
30	1.1	2.9	13	18	5.0	12	14	13	18	21	11
40	1.7	3.6	14	20	6.2	14	16	14	20	23	13
50	2.1	4.0	16	21	7.0	15	17	15	22	24	14
75	2.8	4.7	16	22	7.5	16	17	15	22	24	15
100	3.1	4.9	16	22	7.4	16	17	16	22	24	16
150	2.9	5.0	15	21	6.4	15	15	15	19	22	14
200	2.6	4.8	14	19	5.3	14	14	14	17	21	13
300	2.0	4.5	12	16	4.1	12	11	12	14	18	12
Unc.	80%	9%	9%	9%	22%	8%	9%	11%	9%	11%	13%

TABLE III. Values of  $\sigma_{21}$  for  ${}^3\text{He}^{2+}$  collisions. Units are  $10^{-20} \text{ m}^2$ .

Energy (keV/u)	He	Ne	Ar	Kr	H <sub>2</sub>	N <sub>2</sub>	CO	O <sub>2</sub>	CH <sub>4</sub>	CO <sub>2</sub>	H <sub>2</sub> O
5	0.50	2.7	9.2	22	5.1	9.5	13	6.0	10	11	9.0
7.5	0.75	3.9	11	21	7.3	11	14	7.5	12	12	11
10	1.1	4.7	12	20	9.0	11	14	8.3	13	13	12
15	2.0	5.3	12	19	10	12	14	9.2	14	14	12
20	2.7	5.2	12	17	10	12	13	9.3	13	13	11
30	3.2	4.6	10	14	8.4	10	10	8.7	11	11	9.0
40	3.0	4.0	8.4	11	6.4	8.7	8.5	7.7	9.2	9.3	7.4
50	2.5	3.5	6.9	9.2	4.7	7.3	6.9	6.5	7.4	7.9	6.3
75	1.7	2.6	4.2	5.5	2.1	4.7	4.3	4.5	4.6	5.6	4.1
100	1.0	2.1	2.7	3.5	0.98	3.2	2.9	3.1	2.7	4.0	1.9
150	0.48	1.4	1.3	1.6	0.27	1.6	1.5	1.6	1.0	2.3	1.5
Unc.	13%	14%	14%	23%	11%	12%	12%	16%	12%	12%	12%

TABLE IV. Values of  $\sigma_{20}$  for  ${}^3\text{He}^{2+}$  collisions. Units are  $10^{-20} \text{ m}^2$ .

Energy (keV/u)	He	Ne	Ar	Kr	H <sub>2</sub>	N <sub>2</sub>	CO	O <sub>2</sub>	CH <sub>4</sub>	CO <sub>2</sub>	H <sub>2</sub> O
5	1.4	2.1	3.2	3.9	0.20	2.7	3.2	3.6	1.5	3.1	2.0
7.5	1.3	2.0	3.1	3.9	0.39	3.1	3.4	3.6	2.1	3.4	2.8
10	1.3	1.8	3.0	4.0	0.52	3.3	3.4	3.6	2.4	3.5	3.1
15	1.2	1.6	2.8	3.9	0.61	3.4	3.2	3.2	2.5	3.6	3.0
20	1.0	1.4	2.4	3.5	0.63	3.3	2.9	2.9	2.3	3.4	2.7
30	0.83	1.2	1.7	2.7	0.54	2.5	2.3	2.2	1.7	2.6	2.0
40	0.64	0.92	1.2	2.0	0.41	1.9	1.6	1.6	1.2	2.0	1.4
50	0.49	0.73	0.81	1.4	0.26	1.4	1.2	1.1	0.81	1.6	0.98
75	0.23	0.40	0.31	0.59	0.068	0.56	0.48	0.46	0.31	0.81	0.40
100	0.086	0.22	0.11	0.27	0.017	0.25	0.22	0.20	0.10	0.35	0.19
150	0.0079	0.09	0.0079	0.067	0.0036	0.055	0.031	0.047	0.0040	0.049	0.029
Unc.	15%	19%	13%	19%	13%	19%	14%	15%	12%	12%	16%

and  $\sigma_{20}$  the uncertainty in the beam collection was 3%, in the effective path length 7%, and in the secondary-emission coefficients 7%. The combined uncertainty for these cross sections was then 11%.

In addition to these uncertainties, there were random errors which we determined by calculating the average deviations from the smooth curves drawn through the average of the points. These deviations were quite different for different target gases. The combined uncertainties including these random errors are given for each gas in Tables I–IV.

#### DATA ADJUSTMENT

As in the earlier  $\text{He}^+$  work, we took advantage of the fact that all four cross sections were measured to make adjustments to them based on the fact that they must be related by the conservation of charge.<sup>17</sup> In this case the relation is

$$\sigma_+ = \sigma_0 + \sigma_{21} + 2\sigma_{20}, \quad (1)$$

assuming that capture of three electrons is negligible. A weighted least-squares adjustment was made to all four cross sections at each energy which minimized the fractional adjustments required to satisfy Eq. (1). The weights were chosen to be the reciprocals of the estimated uncertainties in the measurements. These uncertainties, which included both systematic and random errors, were calculated separately for each combination of gas target and type of cross section, but were assumed to be the same for all beam energies. These uncertainties are given with the final results. In no case did the adjustment exceed the assigned uncertainty.

#### EXPERIMENTAL RESULTS

Figures 1–4 show the original data for several of the targets along with the lines representing the smoothed and adjusted final results. The final results are also given in Tables I–IV along with the estimated uncertainties for each case. Figures 5–8 show a comparison of the present results with what previous data was available.

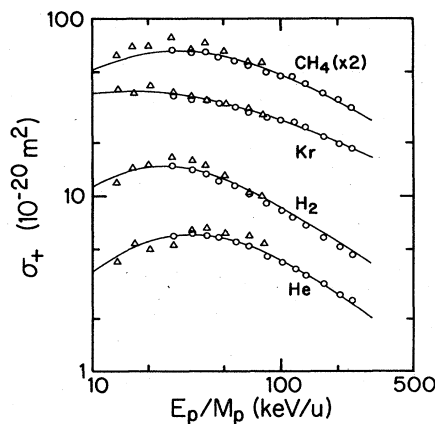


FIG. 1. Values of  $\sigma_+$  for  ${}^3\text{He}^{2+}$  on methane, krypton, hydrogen, and helium. Unadjusted data from the low-energy accelerator are shown as triangles and from the high-energy accelerator as circles. Lines represent the final adjusted data. (See text.)

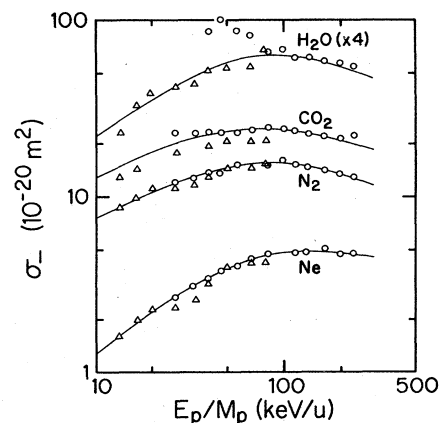


FIG. 2. Values of  $\sigma_-$  for  ${}^3\text{He}^{2+}$  on water vapor, carbon dioxide, nitrogen, and neon. Symbols as in Fig. 1.

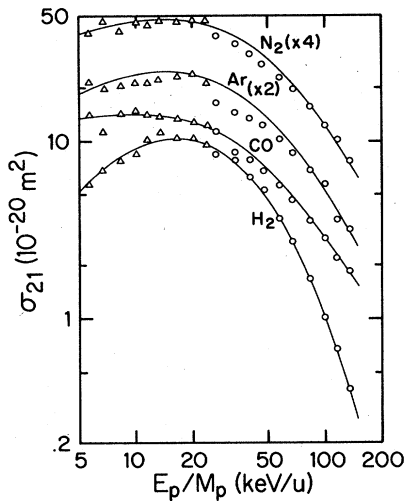


FIG. 3. Values of  $\sigma_{21}$  for  ${}^3\text{He}^{2+}$  on nitrogen, argon, carbon monoxide, and hydrogen. Symbols as in Fig. 1.

1. *Helium.* Our  $\sigma_+$  data are in good agreement with that of Puckett, *et al.*,<sup>12</sup> as seen in Fig. 5, but our  $\sigma_-$  data are 8–39% higher. (See Fig. 6.) Unfortunately, our  $\sigma_-$  measurement in helium had a very large uncertainty and since the apparatus had been reconfigured for another experiment, it was not feasible to recheck the data. The  $\sigma_{21}$  and  $\sigma_{20}$  data are in reasonably good agreement with the average of earlier data (see Figs. 7 and 8), except for the  $\sigma_{20}$  cross sections which are somewhat lower than that of Pivovar *et al.*<sup>10</sup> at the highest energies.

2. *Neon.* There does not appear to be any previous ionization data in the present energy range. Latypov *et al.*,<sup>1,5</sup> have presented  $\sigma_+$  data up to 2 keV/u which appears to be about 5 times too large to extrapolate smoothly to our data. It is likely that their neon cross sections are in error since their neon cross sections are even larger than the ones they give for argon. We are in fair agreement with

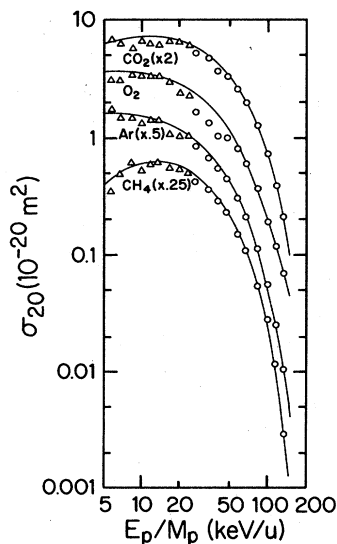


FIG. 4. Values of  $\sigma_{20}$  for  ${}^3\text{He}^{2+}$  on carbon dioxide, oxygen, argon, and methane. Symbols as in Fig. 1.

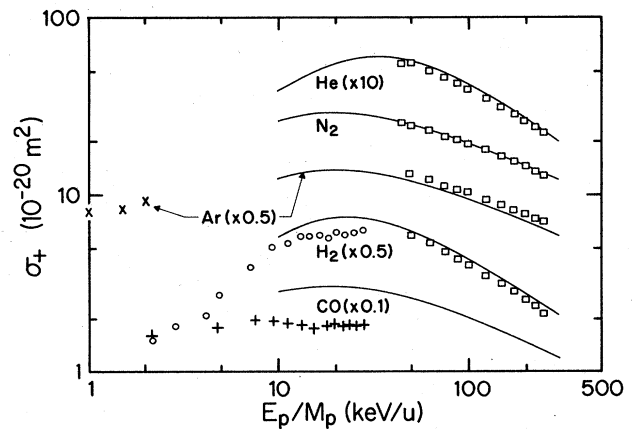


FIG. 5. Comparison of present  $\sigma_+$  data, shown as lines, with data of other investigators. Graham *et al.* (Ref. 13),  $\circ$  and  $+$ ; Latypov *et al.* (Ref. 15),  $\times$ ; Puckett *et al.* (Ref. 12),  $\square$ .

Baragiola and Nemirovsky's neon charge-transfer data,<sup>5</sup> but cannot confirm the structure which they report.

3. *Argon.* As shown in Figs. 5 and 6, the present  $\sigma_+$  and  $\sigma_-$  data are 5–10% lower than that of Puckett *et al.*<sup>12</sup> but this discrepancy is within the combined error bars of the two experiments. It appears that our  $\sigma_+$  cross sections, if extrapolated, would be in reasonable agreement with the data of Latypov *et al.*<sup>15</sup> as seen in Fig. 5. There are discrepancies of considerable magnitude among the reported values of the charge-transfer cross sections. Our  $\sigma_{21}$  cross sections are in reasonable agreement with those of Shah and Gilbody<sup>1</sup> at low energy and with those of Pivovar *et al.*<sup>9,10</sup> at high energy as seen in Fig. 7. Our  $\sigma_{20}$  data are in good agreement with Shah and Gilbody<sup>1</sup> at low energy but are lower than Pivovar *et al.*<sup>10</sup> at high energy.

4. *Krypton.* There apparently are no previous ionization data for krypton in this energy range. The lower-energy work of Latypov *et al.*<sup>15</sup> appears to extrapolate

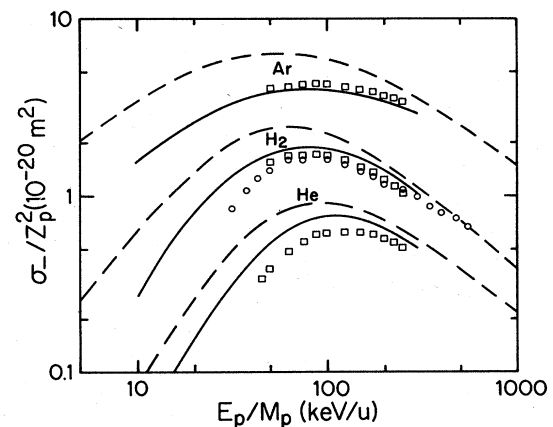


FIG. 6. Comparison of present  $\sigma_-$  data, shown as solid lines, with data of other investigators. Shah and Gilbody (Ref. 14),  $\circ$ . Other symbols as in Fig. 5. Dashed lines are data from  $\text{H}^+$  collisions from Rudd *et al.* (Ref. 18).

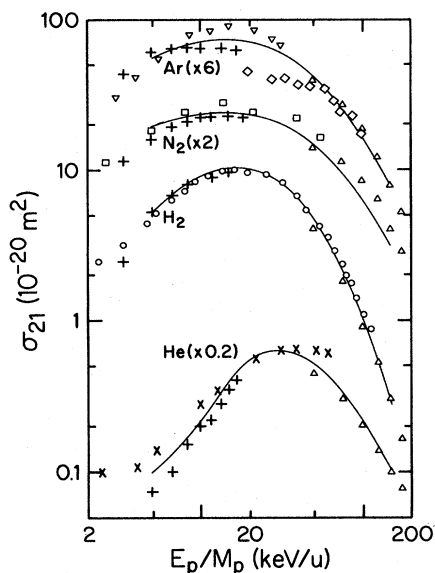


FIG. 7. Comparison of present  $\sigma_{21}$  data, shown as solid lines, with data of other investigators. Baragiola and Nemirovsky (Ref. 6),  $\diamond$ ; Berkner *et al.* (Ref. 8),  $\times$ ; Stearns *et al.* (Ref. 7),  $\square$ ; Bayfield *et al.* (Ref. 4),  $\nabla$ ; Pivovar *et al.* (Refs. 9 and 10),  $\triangle$ ; Shah and Gilbody (Refs. 1 and 2),  $\circ$  and  $+$ .

well to our data, however. The present  $\sigma_{21}$  and  $\sigma_{20}$  data agree reasonably well with that of Shah and Gilbody<sup>1</sup> and with Pivovar *et al.*<sup>9,10</sup> Figure 8 shows the  $\sigma_{20}$  data.

5. *Hydrogen.* Our  $\sigma_-$  data agree fairly well with that of Puckett *et al.*<sup>12</sup> and with Shah and Gilbody<sup>14</sup> at high energies, but are as much as 50% higher than the latter at the lowest energy as seen in Fig. 6. As seen in Fig. 5, the  $\sigma_+$  data are in agreement with that of Puckett *et al.*<sup>12</sup> but are 15–25% higher than that of Graham *et al.*<sup>13</sup> Our

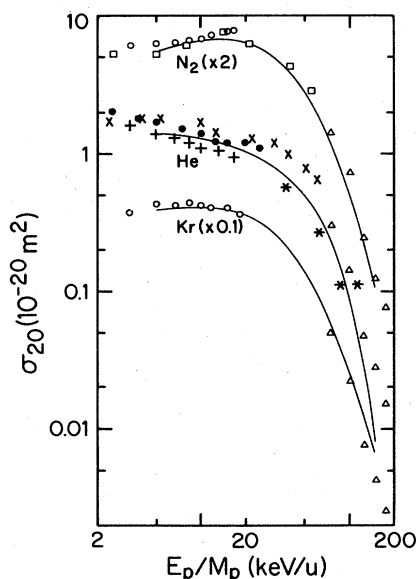


FIG. 8. Comparison of present  $\sigma_{20}$  data, shown as solid lines, with data of other investigators. Allison (Ref. 11),  $*$ ; Afrosimov *et al.* (Ref. 5),  $\bullet$ . Other symbols as in Fig. 7.

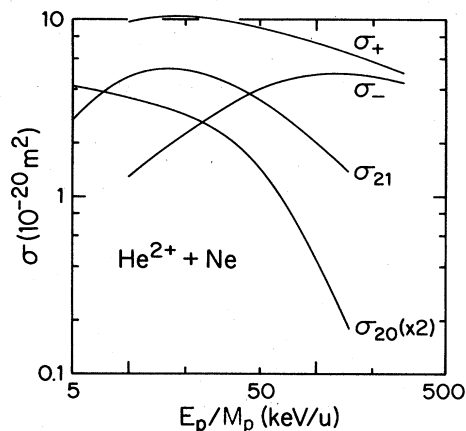


FIG. 9. Comparison of the four measured cross sections for neon. The top curve is the sum of the bottom three.

$\sigma_{21}$  cross sections are in excellent agreement with those of Shah and Gilbody as shown in Fig. 7, but our  $\sigma_{20}$  data tend to be higher than theirs at low energy and lower at high energy.

6. *Nitrogen.* The present  $\sigma_+$  and  $\sigma_-$  measurements are both in excellent agreement with those of Puckett *et al.* in the region of overlap. See Fig. 5. The capture data are in generally good agreement with earlier work (see Figs. 7 and 8) except that  $\sigma_{20}$  falls somewhat below that of Pivovar at high energies.

7. *Oxygen.* There are no oxygen-ionization data with which to compare. The capture data agree fairly well with Shah and Gilbody<sup>1</sup> except that the energy dependence is somewhat different for  $\sigma_{21}$ .

8. *Carbon monoxide.* The  $\sigma_+$  data of Graham *et al.* is 50–65% lower than our data in the 10–30 keV/u region where they overlap. This is seen in Fig. 5. Also the energy dependences are somewhat different. No other data are available for carbon monoxide, but the agreement with the nitrogen data is an indication of its accuracy.

9. *Carbon dioxide, methane, water vapor.* No previous data for any of the cross sections for these gases is known. In Fig. 2 the  $\sigma_-$  data for water vapor taken on the high-energy accelerator appears anomalously high, near 50 keV/u. As with the helium data, it was not possible to re-take this data on that accelerator. However, the data taken on the low-energy accelerator did not confirm these large values and, except for their effect on the stated error, they were ignored. This anomaly could have been due to difficulties in controlling the beam near the low end of that accelerator's energy range.

In Fig. 6 the present  $\sigma_-$  data are also compared with the proton impact data of Rudd *et al.*<sup>16</sup> The abscissa is projectile energy per unit mass and thus compares projectiles at equal velocities. The ordinate is the cross section divided by the square of the projectile charge. According to the Born approximation, when compared in this way, the cross sections should be the same for all bare nuclei. It is clear that  $Z_p^2$  scaling is not accurate at low energies, but at the higher energies the cross sections tend to converge as expected. DuBois<sup>18</sup> has shown that a sizable

fraction of the electrons are ejected simultaneously with electron capture. These second-order processes, which are most important at energies below 100–200 keV, would not be expected to scale as  $Z_p^2$ .

In Fig. 9 we show all four  $\text{He}^{2+}$  cross sections for neon. From Eq. (1), the lower three curves all add up to equal  $\sigma_+$ , the top curve. It is seen that ion production is dom-

inated by electron ejection at the higher energies, but by charge-transfer processes at lower energies.

#### ACKNOWLEDGMENTS

This paper is based on work performed under National Science Foundation Grants Nos. PHY80-25599 and PHY-8401328.

\*Present address: 3 Eglantine Park, Hillsborough, County Down BT26 6HL, North Ireland.

<sup>1</sup>M. B. Shah and H. B. Gilbody, *J. Phys. B* **7**, 256 (1974).

<sup>2</sup>M. B. Shah and H. B. Gilbody, *J. Phys. B* **11**, 121 (1978).

<sup>3</sup>W. G. Graham, C. J. Latimer, R. Browning, and H. B. Gilbody, *J. Phys. B* **7**, L405 (1974).

<sup>4</sup>J. E. Bayfield and G. A. Khayrallah, *Phys. Rev. A* **11**, 920 (1975).

<sup>5</sup>V. V. Afrosimov, G. A. Leiko, Yu. A. Mamaev, and M. N. Panov, *Zh. Eksp. Teor. Fiz.* **67**, 1329 (1974) [*Sov. Phys.—JETP* **40**, 661 (1975)].

<sup>6</sup>R. A. Baragiola, and I. B. Nemirovsky, *Nucl. Instrum. Methods* **110**, 511 (1973).

<sup>7</sup>J. Warren Stearns, Klaus H. Berkner, Vincent J. Honey, and Robert V. Pyle, *Phys. Rev.* **166**, 40 (1968).

<sup>8</sup>Klaus H. Berkner, Robert V. Pyle, J. Warren Stearns, and John C. Warren, *Phys. Rev.* **166**, 44 (1968).

<sup>9</sup>L. I. Pivovarov, V. M. Tubaev, and M. T. Novikov, *Zh. Eksp.*

*Teor. Fiz.* **41**, 26 (1961) [*Sov. Phys.—JETP* **14**, 20 (1962)].

<sup>10</sup>L. I. Pivovarov, M. T. Novikov, and V. M. Tubaev, *Zh. Eksp. Teor. Fiz.* **42**, 1490 (1962) [*Sov. Phys.—JETP* **15**, 1035 (1962)].

<sup>11</sup>S. K. Allison, *Phys. Rev.* **109**, 76 (1958).

<sup>12</sup>L. J. Puckett, G. O. Taylor, and D. W. Martin, *Phys. Rev.* **178**, 271 (1969).

<sup>13</sup>W. G. Graham, C. J. Latimer, R. Browning, and H. B. Gilbody, *J. Phys. B* **7**, L405 (1974).

<sup>14</sup>M. B. Shah and H. B. Gilbody, *J. Phys. B* **15**, 3441 (1982).

<sup>15</sup>Z. Z. Latypov, I. P. Flaks, and A. A. Shaporenko, *Zh. Eksp. Teor. Fiz.* **57**, 29 (1970) [*Sov. Phys.—JETP* **30**, 29 (1970)].

<sup>16</sup>M. E. Rudd, R. D. DuBois, L. H. Toburen, C. A. Ratcliffe, and T. V. Goffe, *Phys. Rev. A* **28**, 3244 (1983).

<sup>17</sup>M. E. Rudd, T. V. Goffe, A. Itoh, and R. D. DuBois, *Phys. Rev. A* **32**, 829 (1985).

<sup>18</sup>R. D. DuBois, *Phys. Rev. Lett.* **52**, 2348 (1984).